We are IntechOpen, the world's leading publisher of Open Access books Built by scientists, for scientists

6,900
Open access books available

186,000
International authors and editors

200M
Downloads

Our authors are among the

154
Countries delivered to

TOP 1%
most cited scientists

12.2%
Contributors from top 500 universities

CLARIVATE ANALYTICS

BOOK CITATION INDEX

INDEXED

WEB OF SCIENCE™

Selection of our books indexed in the Book Citation Index
in Web of Science™ Core Collection (BKCI)

Interested in publishing with us?
Contact book.department@intechopen.com

Measurement of Multiphase Flow Characteristics Via Image Analysis Techniques: The Fluidization Case Study

Antonio Busciglio, Giuseppa Vella and Giorgio Micale
Università degli Studi di Palermo
Italy

1. Introduction

In recent years, thanks to the continuous development of digital imaging systems and digital image processing, a great number of researchers have chosen digital visual methods to be applied in the field of experimental fluid dynamics. These kinds of techniques play a fundamental role in analysis and data acquisition for multiphase flows such as gas-solid, gas-liquid, solid-liquid flows, where the observation of inter-phase boundaries is relatively simple.

In this chapter, an overview on some imaging-based experimental techniques for the analysis of complex multiphase systems is reported. In particular, some techniques aimed at the study fluidization dynamics will be analyzed and discussed, as developed by our research group.

Fluidization occurs when the forces exerted by a fluid passing through a bed of particles counteract the particle weight. At this stage, the bed on the whole is just supported by the flowing gas and acquires fluid-like properties, free to flow and deform, keeping a horizontal level when tilted and allowing low-density objects to float on the bed surface. For most of the cases of gas-solid fluidization, fluid velocity increments beyond incipient fluidization are accompanied by the formation of bubbles, or cavities with hardly any solid particles in them. In general, gas flow beyond incipient fluidization mostly reports to bubble flow. Aggregation of solid particles into a dense continuous phase, making room for the passage of most of the gas in excess of incipient fluidization through a bubbling discontinuous phase, bespeaks the two phase nature of gas-solid fluidization. Such a phenomenon of gas-solid systems was designated aggregative.

Much has been written about bubbling phenomena in fluidized beds over the last years. In fact a good understanding of the bubble hydrodynamics is necessary to understand bubble-related phenomena such as solid mixing and segregation, reaction conversion, heat transfer and particle entrainment in beds operated in the bubbling regime. The size, shape and velocity of bubbles and relevant flow patterns are of key interest in bubbling hydrodynamics.

The adoption of image analysis techniques can be in principle fully automated and made robust for measurement of the complex fluid dynamic behavior of fluidized systems. By in-house development of a suitable software, it is possible to get a total control over every single step of the procedure and every single parameter involved in the calculations, thus achieving a higher level of reliability of the data so far obtained. Thanks to the high level

of automation, it is possible to simultaneously compute a large number of data, allowing at the same time a meaningful statistical analysis that is intrinsically necessary given the chaotic nature of the source data.

The first technique reported is an original technique based on the back-lighting of 2-dimensional fluidized bed for the measurement of gas bubbles rising up through the dense granular phase of a fluidized bed. The main problems during the development of this particular technique are due to the set up of the light panel, and the setting up of camera, in order to obtain the best level of contrast between bubbles and emulsion phase, limiting in any case the possible over-exposition of images. Moreover, some care must be taken in the choice of threshold values for the discrimination of bubble phase from emulsion phase. A careful choice of camera setting allows to perform measurement of time dependent quantities (for which high image acquisition rates are generally necessary) and quasi-steady state properties measurements (for which, conversely, long experiments times and low image acquisition rates can be used). After data acquisition, a number of examples of derived quantities measured will be shown, together with the basic principles adopted for the derivation. Of course, most of the examples are here reported for the case of fluidized beds, but could be adapted for the measurement of other multiphase systems.

The second technique here reported allows the measurement of the solid phase behavior in a bubbling fluidized bed, by means of front-lighting of a granular bed of glass white particles in which a small amount of black corundum particles are dispersed as a seed for the application of a velocimetry technique akin to the PIV technique used for flow field measurement in single phase systems. The main problems encountered are connected with the set-up of a fast acquisition system and the image processing, in order to isolate the motion of tracers for subsequent velocity measurements.

The third technique here reported deals with the measurement of mixing pattern and dynamics measurements of two differently colored particles (having the same density but different size), allowing for the first description of mixing dynamics of the bed with non-intrusive technique. The main problems to be faced are due to the solid-phase occupied pixels identification and in the translation of luminance data into mixing-extent data. This shall pass through advanced color-image analysis.

2. Experimental set-up

For the case study here presented 2-D fluid-bed reactor was adopted in order to attain full visualization of the flow characteristics within the bed itself. The adoption of a 2D bed, in which bed thickness is quite smaller than the other dimensions allows easy visualization of bubble dynamics and solid-phase dynamics, as will be further discussed in the following sections devoted to the presentation of imaging techniques. Moreover, 2D data can be readily used for the validation of CFD codes and models (Busciglio et al., 2009) without the need for full 3D, time-consuming simulations.

The 2D fluid-bed facility reactor (size: 250 (w) x 1200 (h) x 10(t) mm) adopted for the experiments presented in this contribution is made of aluminium and equipped with glass walls at front and back. Sintered plastic porous distributor is placed at the bottom of the particle bed, providing large enough pressure drop to avoid dynamic coupling between gas fluxes within the bed and the wind box placed below the distributor to guarantee uniform gas distribution. Further details on the gas supply system can be found elsewhere (Busciglio et al., 2008). The settled bed height was generally set to twice the bed width.

For the measurement of bubbling dynamics characteristics or emulsion phase velocity, experimental data (i.e. bed images) were acquired after full steady state was achieved, in order to avoid measuring bubble behavior during the initial mixing of powders. Conversely, for the measurement of mixing dynamics of powder mixtures, images were taken of the mixing transient itself, in a condition very far from steady state that will be discussed more in detail in the following. In all cases, the observation was focused on the whole bed, without selecting any particular region of interest, to allow a full field analysis of the fluidization dynamics.

The bubble-related flow structures were visualized with the aid of a back-lighting device and recorded by a digital camcorder (mvBlueFox 121c), placed opposite to the bed. Continuous high intensity uniform illumination was obtained by placing six fluorescent lamps at the back side of the bed. The experimental system was also equipped for high intensity front-lighting of the bed, that was adopted for the measurement of solid-phase related measurement (mixing dynamics and velocity field). In the case of front-lighting, a careful positioning of the lamps (often coupled with the adoption of some kind of diffusing-light device) is needed to avoid any shadow or refection that could infer the measurements. Conversely, this problem is practically non-existent when back-lighting is adopted.

The digital visual acquisition system allowed to collect images of the bed at different frequencies ranging from 1 to 70 fps, see Fig.1. The choice of the correct frame rate mainly depends on the time scale of the phenomena under investigation. As an example, bubble characterization needs the lowest frame rate, in order to take images of different bubbles instead of different images of the same bubble rising through the bed. Conversely, bubble velocity measurements need large frame rates, in the order of 30 to 60 fps, in order to make bubble tracking algorithm (that is able to follow the the same bubble in different subsequent frames) reliable enough.
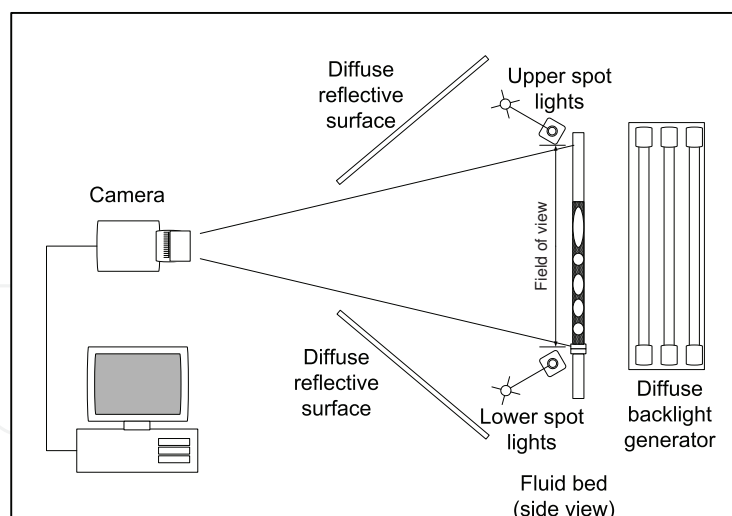

Fig. 1. Fluid bed experimental set-up: optical scheme.

In all cases, the flow dynamics were analyzed and processed using purposely developed digital image analysis routines. In order to automate the image acquisition and data processing procedure, all in-house routines were developed using the Matlab image processing toolbox.

3. Bubbles measurements

Mixing of powders and solid-fluid contact efficiency within the bed is driven by the particle-free voids of bubbles that form when the gas flow rate exceeds the superficial velocity of minimum bubbling. The bubbles ensure that the particles are circulated throughout the bed so that properties and process condition could be considered as uniform.

Many characteristic features of fluidized beds, as well as the fluidization quality in general, are highly dependent on the distribution of bubbles and their physical properties. Therefore the measurement of bubble characteristics and their distribution over the entire cross-section of fluidized beds is of great practical importance in understanding the overall fluid dynamics of the reactors as this is necessary for their design and scale-up. In particular bubble size, velocity, shapes and flow patterns are of key interest in bubbling hydrodynamics. These properties have been extensively measured experimentally by various methods. The experimental methods and finding have been summarized in several review articles (Cheremisinoff, 1986; Davidson et al., 1985).

Different techniques have been employed to experimentally measure bubble parameters. These can be broadly classified into two categories depending on the nature and position of the sensors used: (i) intrusive techniques and (ii) non-intrusive techniques. The intrusive techniques such as resistance, inductance, impedance, piezoelectric or thermal probes were extensively used and could provide accurate measurements. However such probes were expected to alter the nature of local fluidization due to their intrusiveness and moreover they were required to move through the whole volume of the fluidized bed in order to map the entire flow field of the reactor. Conversely, non intrusive techniques enable good visual observation without interfering with fluidization dynamics. These include photographic, X-ray radiography, light scattering, laser techniques, positron emission tomography, electrical capacitance tomography, optical tomography, ultrasonic tomography, positron emission particle tracking and particle image velocimetry.

In recent years a great number of researchers have chosen digital visual methods to be applied in the field of experimental fluid dynamics (Boemer et al., 1998; Gera & Gautam, 1995; Hull et al., 1999; Lim & Agarwal, 1990; Mudde et al., 1994). This technique results an important method, in particular for the analysis of bubble properties, as it provides rigorous and detailed information about the flow structure of the entire bed without interfering with flow dynamics. Digital visual methods can only be effectively used in pseudo-two-dimensional beds, as in this case bubbles can be easily observed. The use of Digital Image Analysis Technique (DIAT) in fluidized bed studies was pioneered by Lim and co-workers (Lim & Agarwal, 1992; Lim et al., 1990; 1993) and their works were summarized by Agarwal et al. (1997).

Hull et al. (1999) reported an experimental data on bubble characteristics averaged size and rise velocity were obtained using digital image analysis method from two-dimensional (thin) bubbling fluidized beds with and without simulated horizontal tube bundles. These data were used to develop semi-empirical correlations for bubble size and rise velocity. Caicedo et al. (2003) used image analysis technique to show that bubble aspect ratio and shape factor in a 2D gas-solid fluidized bed where in generally normally distributed. A wider experimental campaign was performed by Shen et al. (2004) an original image analysis technique. The authors were able to measure several bubble properties such as size and rise velocity, axial and radial distribution of bubbles and gas through flow, in order to develop suitable correlations for bubble diameter and rise velocity in 2D beds.

In the late works by Lim and co-workers (Lim et al., 2006; 2007), digital image analysis was adopted to study bubble void fraction in the frequency domain and together with relevant statistical analysis, showing how frequency-domain statistics could be useful for inferring the bed fluidization quality.

In the paper by Busciglio et al. (2008), digital image analysis technique was developed to study the hydrodynamics of a two dimensional bubbling fluidized bed. The technique allows for the simultaneous measurements of the most significant bubble properties, *i.e.* bubble size and bubble velocity distributions, bed height and bubble-phase hold-up, by means of a purposely developed software. Notably, the same authors (Busciglio et al., 2009) applied successfully their technique to both experimental data and, for the first time, to computational results, as obtained by a commercial CFD code. In particular, the use of the very same data analysis technique to both sets of data allows for a fully consistent quantitative comparison of the very same physical quantities, overcoming the well known problem of comparison sensitivity to the differences in the experimental measurement techniques and numerical post-processing computations.

Laverman et al. (2008) studied the hydrodynamics of an experimental freely bubbling pseudo 2-D fluidized bed coupling Particle Image Velocimetry and Digital Image Analysis. This technique allowed to investigate the mutual interaction between the bubble and emulsion phase in detail. Similar techniques, in which PIV and image analysis techniques were coupled together were also adopted by Sánchez-Delgado et al. (2008) and Sánchez-Delgado et al. (2010)

The work by Asegehegn and co-workers (Asegehegn et al., 2011a;b) used a back-lighting based image analysis technique to study 2D gas fluidized beds with and without a dense tube bank, comparing by means of the same technique both experimental and numerical results.

3.1 Image analysis technique

The aim of the present section is to present the technique used for the analysis of bubbling fluidization on the basis of digital image processing. The digital image analysis technique (DIAT) developed comprises acquiring images using a camcorder and then processing and analyzing the images using an in-house routine. The in-house routine was developed with the help of the Matlab 7.3 (The MathWorks inc.), using the Image Processing Toolbox to fully automate the procedure of image processing.

Bubbles were detected because they transmit light emitted at the back of the bed which reaches the camera. Thus white areas represent bubbles while the remaining black area indicates the emulsion phase, as can be clearly seen in Fig.2.

Once recalled the image to analyze, the routine works through some simple steps:

- Thresholding of the original RGB image to obtain a binary image of the bed. This allows the discrimination of the bubble phase from the dense phase of the bed;
- Indexing of all individual regions inside the area of interest;
- Filtering of false bubbles and peripheral voids;
- Property recording of each region inside the area of interest.

In particular the thresholding procedure is used to transform a greyscale image (in which any pixel assumes values ranging from 0 to 1) into a binary one, suitable for object identification. This is an important step in discriminating a bubble from the rest of the bed. Bubble
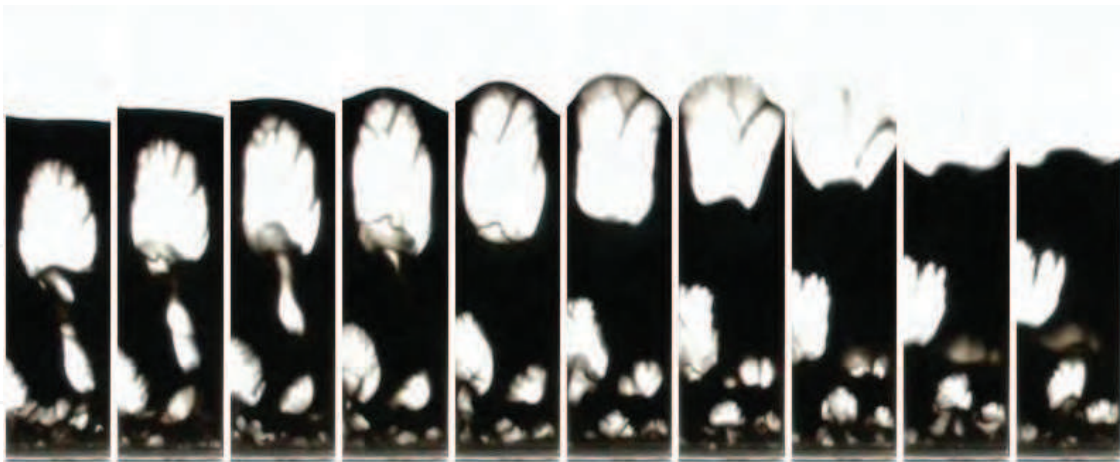
Fig. 2. Typical snapshot sequence obtained by bed back-lighting (glass particles, $U = 0.18\,m/s$, $d_p = 212 - 250\,\mu m$).

discrimination is usually done with the help of a threshold value for the pixel intensity of the grayscale images. The problem is thus converted in finding a correlation between pixel luminance, ranging from 0.0 to 1.0 and voidage, ranging from 0.4 to 1.0. The conventional distinction between the emulsion phase and the bubble phase is set at a voidage value of 0.80 (Yates et al., 1994). If the relation between luminance and voidage were assumed linear, a luminance threshold value of about 0.67 would be used. However a linear correlation does not hold true in describing the phenomenon of light transmission across a fluid bed, where typically a Beer-Lambert law applies (Boemer et al., 1998; Brucato & Rizzuti, 1997a;b; Rizzuti & Yue, 1983; Yates et al., 1994; Yue et al., 1986). On the other hand, the very wide and flat valley between the peaks in the bimodal distribution of gray-level, shown in Fig.3, ensures that the choice of any arbitrary value of luminance threshold in the range of $0.4 - 0.8$ influences in a marginal way the bubble property measurements. This is equivalent to use the so called entropy method (Kapur et al., 1985). For the images used in this work, this condition holds true, and the threshold value can be chosen using different considerations. In the left part of Fig.3 a typical gray-scale bed image is shown, while a typical gray level distribution is shown in the center of the same figure. The threshold value, in this case can be chosen at any point in the range of $0.3 - 0.8$, resulting in negligible influence of threshold value on bubble size measurement.

The binary image thus obtained is then subdivided (labeled) into different components, based upon connectivity analysis. For each bubble present in the image, its relevant area, equivalent diameter, and centroids coordinates are computed as reported in Eqns.1 and 2.

$$A_b = \sum b\,(x,y) \tag{1}$$

Bubble centroid coordinates can be computed as follow:

$$x_c = \int \int x b\,(x,y)\,dxdy$$
$$y_c = \int \int y b\,(x,y)\,dxdy \tag{2}$$

where the integrals are extended to the area occupied by the analyzed bubble. Equivalent diameter is then calculated from the knowledge of bubble area.
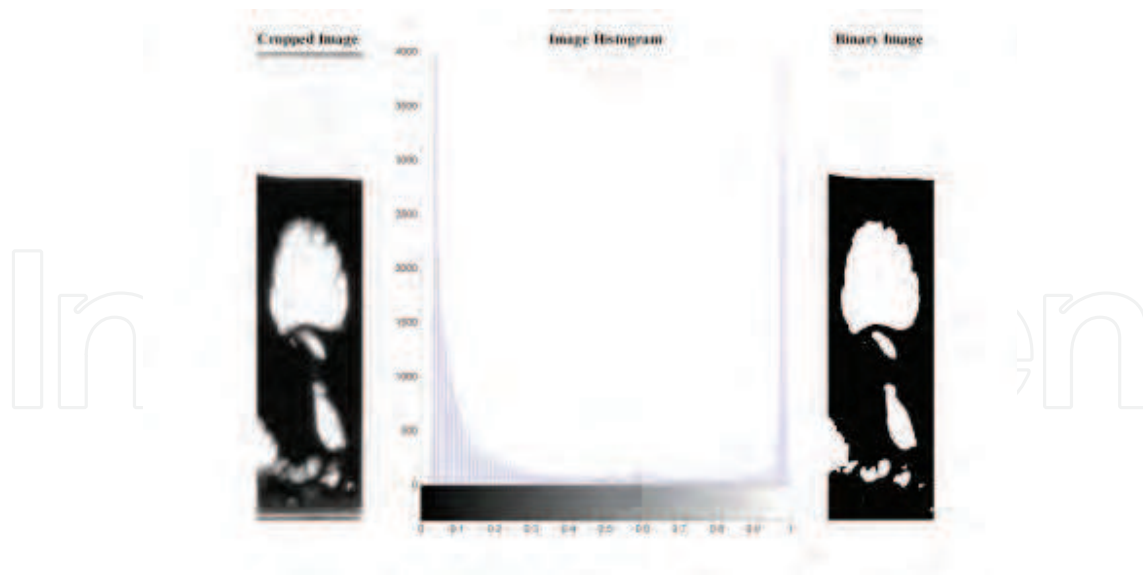
Fig. 3. Original image (left), gray level histogram (center) and threshold image (right).

Distances and areas expressed in pixels can be easily converted in metric distances and areas by multiplying with suitable scale factors preliminarily determined by a set of still calibration images. Notably, for bubble size and position measurement, very low values of frame rate can be adopted, typically 1 fps, in order to avoid measuring the same bubble in different positions within the bed.

Filtering of false bubbles is necessary because of the recirculation of solid particles inside each bubble rising through the bed. In high contrast images, this phenomenon appears in the form of high solid concentration zones at the bottom of the bubble. In the thresholding step this can lead to the appearance of a bubble followed by a constellation of small bubbles following the first one at the same velocity. The presence of the above mentioned false bubbles and peripheral voids, *i.e.* rising voids adherent to the lateral walls and bubbles bursting at the top of the bed, have been carefully excluded from the statistical analysis of bubble properties.

Once bubble in each frame were analyzed, it is possible to compute bubble velocity. This was accomplished adopting a self developed Lagrangian Velocimetry Technique (LVT), (Busciglio et al., 2008). The Lagrangian velocimetry technique (*LVT*) developed uses a very simple tracking algorithm to follow the displacement of each bubble in two (or more) subsequent frames. Of course, the higher the frame rate, the more accurate the bubble tracking will result. For bubble velocity measurement, a frame rate of 60 fps was found to be well suited.

By adopting the LVT procedure it is possible to obtain:

• Distribution (cloud) of bubble rise velocities and average velocity as function of equivalent diameter;

• Distribution (cloud) of bubble lateral velocities as function of equivalent diameter;

• Distribution of bubble rise angle (probability plot);

• Statistical distribution of velocity coefficients ϕ for each bubble, where the bubble velocity is given by $U_b = \phi(gD_b)^{0.5}$.

Once the bubbles rising up through the bed are indexed, it is possible follow the time evolution of each property of each bubble through its path along the bed.

This quantities alone can not be directly used for bubbling regime characterization, but a further step of data post-processing is needed to assess fluidized bed behavior. In the following, the raw data obtained will be discussed, together with some of the numerical and statistical methods adopted for translation of large amount of raw data into information useful for fluidization quality characterization.

3.2 Typical results

Bed height and overall bubble hold up data are the simplest data to be obtained. In particular, in Fig.4 it is possible to observe the characteristic saw-tooth shaped fluctuations of the free surface of the bed, due to the eruption of bubbles. Bubble hold up data are computed by dividing the sum of bubble projected areas in each frame by the total area occupied by the bed (this last being computed as the overall image area minus the freeboard projected area). It must be observed that the bed expansion dynamic and the relevant bubble hold-up dynamic, even if similar, are linked to rather different phenomena. In fact, overall bed expansion depends on both the extent of the bubble phase content and the average expansion of the emulsion phase (including, for example small non-visible bubbles, and the expanded cloud region surrounding the bubbles), while bubble hold-up measures just bubble overall content within the bed.
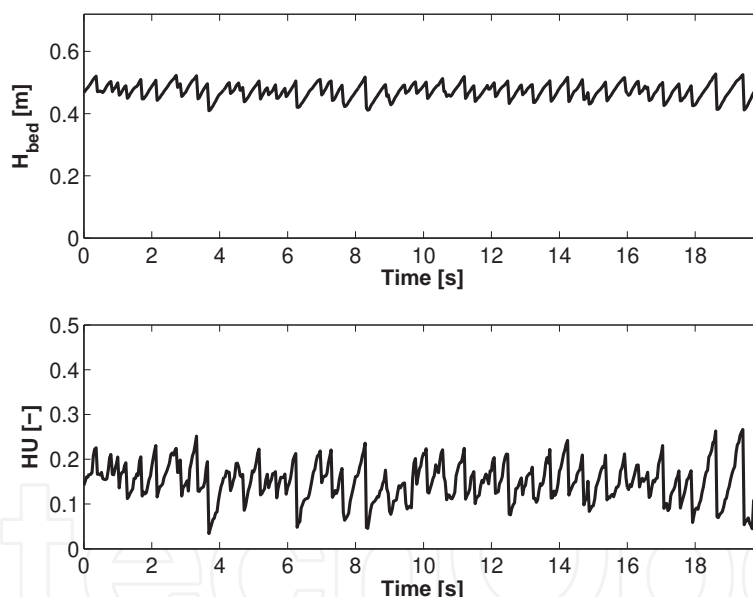

Fig. 4. Typical measurement of bed height and instantaneous average bubble hold-up (glass particles, $U = 0.18\,m/s$, $d_p = 212 - 250\,\mu m$).

Bubble equivalent diameters can be conveniently reported as function of bubble distance from distributor, since bubble size is expected to grow along its path through the bed because of coalescence phenomena. The full set of data are presented in Fig.5(a) in raw cloudy form, in order to highlight the complex bubble behavior along bed height. The adoption of an average curve with indication of its variance would not account for the richness of the raw data. Conversely, the cloudy data presented allow the visualization of the small bubbles that are inside the bed even at the highest elevations, while an average curve, even if with variance, could not show such characteristic and complexity.
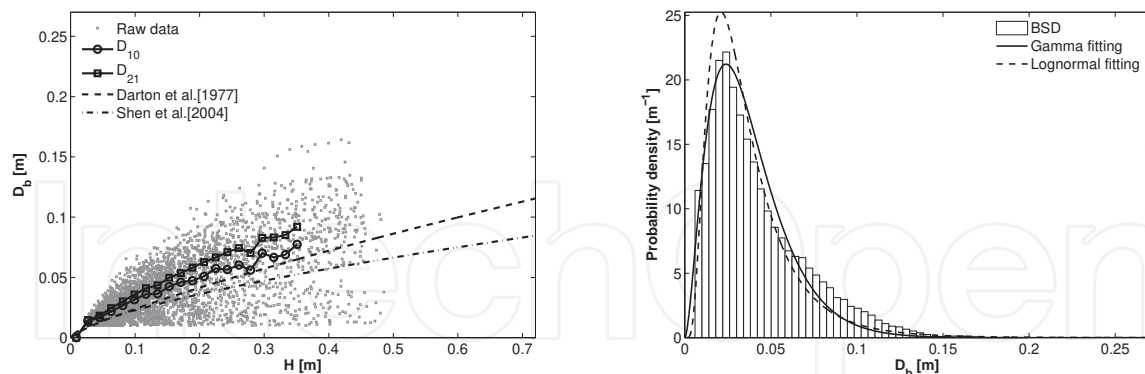
(a) Diameter evolution as a function of the distance above the distributor

(b) Typical bubble size distribution

Fig. 5. Typical measurement of bubble size distributions (glass particles, $U = 0.18\,m/s$, $d_p = 212 - 250\,\mu m$).

On the whole the experimental data show a characteristic increase in bubble diameter, with an upper envelope of data approximately following a power law, in accordance with the analysis by Darton et al. (1977). However, the presence of a wide distribution of bubble sizes is evident at all elevations of the bed, as a result of the splitting and/or nucleation phenomena. This results are in agreement with the finding of Hulme & Kantzas (2004), in which large data scattering on bubble diameter *vs.* distance above the distributor was shown.

A different way for bubbling characterization passes through the analysis of the overall bubble size distribution (BSD). Some experimental distributions of bubble equivalent size distribution on the whole bed are reported in Fig5(b). The experimental distributions show a characteristic positive skewness of the distributions at all inlet gas velocities, in accordance with relevant literature data (Argyriou et al., 1971; Lim et al., 1990; Liu & Clark, 1995; Morooka et al., 1972; Rowe & Yacono, 1975; van Lare et al., 1997; Werther, 1974a;b). Thanks to the huge number of data available from image analysis technique, it is possible to observe that both Gamma and Log-normal distributions generally adopted in literature give rise to poor agreement with the experimental data for bubbles larger than $5\,cm$. This effect is probably linked to an oversimplification of the phenomena, that need more sophisticated analysis techniques to be better characterized (Busciglio et al., 2010).

Once the boundary between emulsion phase and bubble phase has been chosen, as already discussed in relevant chapter, the bubble hold up ϵ_b (or HU) can be simply defined as:

$$\epsilon_b = \frac{\int_V V_b dV}{\int_V V_b dV + \int_V V_{emulsion} dV} \tag{3}$$

To define the local gas hold-up, it is sufficient to define a proper control volume inside the whole system, and computing the limit for control volume towards zero.

$$\epsilon_{b,loc} = \lim_{V \to 0} \frac{\int_V V_b dV}{V} \tag{4}$$

To compute the time averaged local gas hold-up:

$$\epsilon_{b,av,loc} = \frac{1}{T} \int_0^T \lim_{V \to 0} \frac{\int_V V_b dV}{V} \tag{5}$$

If the control volume is infinitesimal, it can not admit the contemporary presence of both phases, thus the local hold up can be replaced with an instantaneous phase indicator:

$$\epsilon_{b,av,loc} \equiv \Phi(x,y) = \begin{cases} 1 \Leftrightarrow (x,y) \in V_{bubble} \\ 0 \Leftrightarrow (x,y) \notin V_{bubble} \end{cases} \tag{6}$$

$$\epsilon_{b,av,loc}(x,y) = \frac{1}{T} \int_0^T \Phi(x,y) \, dt \tag{7}$$

This definition of phase indicator is immediately applicable to compute local time averaged maps of gas hold-up by the means of digital image analysis techniques. We have to consider the images that can be obtained by the image analysis based on binarized images of the back-lighted fluidized bed already described. If we assume to assign to gas-phase occupied pixels a unitary luminance value, and zero luminance value otherwise, it is simple to observe that luminance value $b(x,y)$ exactly coincides with the gas phase indicator $\Phi(x,y)$ above defined.

The analysis of experimental time averaged bubble phase hold-up, shown in Fig.6(a), allows the visual observation of preferential bubble paths along the bed, with a typical reverse-Y shaped pattern starting near the bottom of the bed and developing in the upper regions of the bed. The reverse-Y shaped pattern is due to the coalescence-driven bubble dynamics prevailing after bubble nucleation in the proximity of the distributor in the intermediate region of the bed.
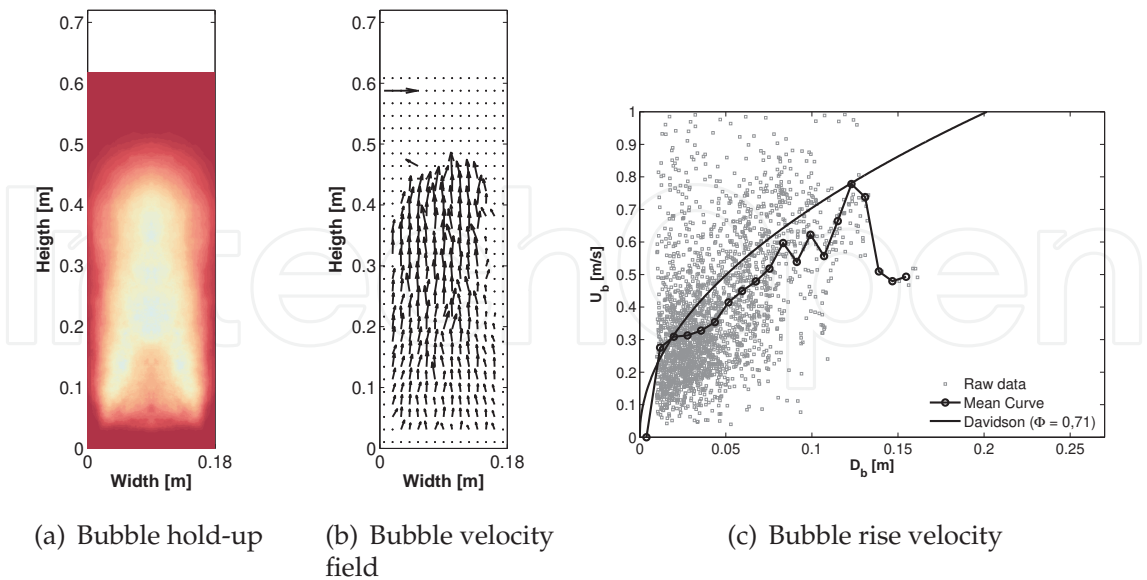

(a) Bubble hold-up   (b) Bubble velocity field   (c) Bubble rise velocity

Fig. 6. Bubble hold-up map and velocity field (glass particles, $d_p = 212 - 250 \, \mu m$, $U = 0.18 \, m/s$).

The analysis of experimental data on average rise velocity as a function of bubble equivalent diameter reported in Fig.6(c) shows a behavior different trend than expectation, *i.e.* than that of the well accepted Davidson equation $u_b = \phi \sqrt{g \, d_b}$. At smaller diameters, the average rise velocities are larger than those predicted, while at the larger diameters the experimental data are quite noisy. In the mid-range of diameters, the data trend follow correctly the square-root law expected, but velocity is somewhat smaller than that deriving form a velocity coefficient of $\phi = 0.71$ as proposed by Darton, and a velocity coefficient of $\phi = 0.58$ should be adopted. These findings can be all explained if the bubbling conditions adopted for experiments are recalled. In a few words, the systems investigated ranged from poorly bubbling to highly slugging system. The more intense the bubbling regime, the stronger are bubble-to-bubble interactions within the bed. On this basis, it is easy to imagine that small bubbles velocities are largely influenced by interaction with larger bubbles, that tend to accelerate them toward coalescence. At the same time, it is clearly very difficult to accurately measure the velocity of large, high-interacting bubbles, because of the chaotic motion of their boundary due to coalescence phenomena, bubble splitting phenomena and deformation along their path along the bed.

The experimental data on bubble rise velocity can also be put in the form of bubble vector plot, as reported in Figs.6(b). The plots can be obtained by suitable time averaging of instantaneous bubble velocity maps. In accordance to the previous discussions, bubble trajectories would be slightly oriented toward the center of the bed in the lower part of the bed and then vertically directed in the upper section of the bed. Moreover, the velocity field plots confirm the evidence for the local bubble hold-up maps shown in Figs.6(a). These latter allow for the visualization of preferential bubble paths along the bed height, whereas the former relates the relevant bubble average velocities to preferential paths.

4. Particle Image Velocimetry

Digital Image Analysis (DIA) and Particle Image Velocimetry (PIV) are two of the most common techniques applied to 2-D fluidized beds to analyze the bubble and emulsion phases. 2-D fluidized beds allow for bubble visualization, making it possible to obtain relevant bubble parameters to characterize the bubbling behavior of the fluidized bed. Additionally, the emulsion phase velocity can be characterized using the PIV technique. PIV is a non-intrusive technique for the measurement of an instantaneous velocity field in one plane of a flow.

In particular Bokkers et al. (2004) studied mixing and segregation induced by a single bubble injected in a fluidized bed at incipient fluidization conditions and in freely bubbling fluidized beds. PIV was applied to obtain the ensemble averaged particle velocity profile in the vicinity of a bubble in dense gas-solid fluidized systems. Laverman et al. (2008) combined the DIA and the PIV techniques to study the bubble behavior (local bubble size and velocity distribution and bubble fraction) and to characterize the emulsion phase profiles (in a pseudo-2-D bed because of the required visual accessibility).

Sánchez-Delgado et al. (2008) presented an experimental study to characterize ascending bubbles and granular velocity in the dense phase of a 2-D fluidized bed. They studied the time-averaged bubble concentration in a 2-Dfluidized bed to characterize the behavior of fluidized beds with different bed aspect ratios and superficial gas velocities. They also applied a PIV method to characterize the particle velocity vectors, collecting information on the location of the recirculation regions within the emulsion phase. The same authors presented also an investigation of the perturbations induced by the bubbles in a 2-D fluidized

bed developing a combination of DIA and PIV (Sánchez-Delgado et al., 2010) to distinguish the dense phase from the bubble phase and obtain the time-averaged velocity of the dense phase as well as the proportion of time that a region was occupied by a bubble.

Particle Image Velocimetry and Digital Image Analysis were used by Agarwal et al. (2011) to study the effect of inlet gas jets located at the distributor in rectangular fluidized beds. Experiments were conducted with varying distributor types and bed media to understand the motion of particles and jets in the grid-zone region of a fluidized bed.

Hernàndez-Jimènez et al. (2011) reported simulation and experimental results of the hydrodynamics of a two-dimensional, bubbling air-fluidized bed. The experimental results have been obtained by means of DIA and PIV techniques applied on a real bubbling fluidized bed to ensure its two-dimensional behavior. This study examines and compares not only the bubble hydrodynamics and dense-phase probability within the bed, but also the time-averaged vertical and horizontal component of the dense-phase velocity, the air throughflow and the instantaneous interaction between bubbles and dense-phase.

In this section we report some details about an original technique adopted for the measurement of the solid phase behavior in a bubbling fluidized bed (based on front-lighting of a granular bed of glass white particles in which a small amount of dispersed black corundum particles) for the application of a velocimetry technique akin to the PIV technique used for flow field measurement in single phase systems.

The PIV technique is able to statistically measure the main particle displacement within two subsequent frames. In traditional PIV the flow is visualized by seeding it with small tracer particles that perfectly follow the flow, in this case the utilized tracer particles are black corundum particles seeding in a granular bed of glass white particles. High intensity front-lighting of the system, coupled with light diffusers (in order to minimize shadows or reflection in the front wall of the bed) and higher frame rates (in the order of $70\,fps$) with respect to those adopted in the case of bubble-dynamic measurement must be adopted. The resulting typical images are reported in Fig.7. Notably, in the rear wall of the bed a yellow panel was placed in order to better isolate bubble-occupied pixels.

| (a) | (b) | (c) | (d) | (e) | (f) |
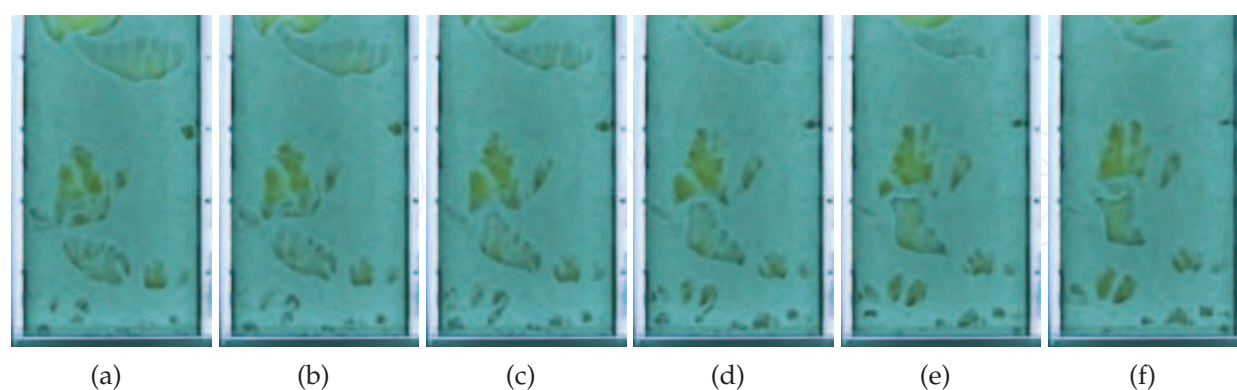
Fig. 7. Snapshot sequence of a PIV-ready fluidized bed taken at $\Delta t = 1/70\,s$, (glass particles with corundum tracers, $U = 0.27\,m/s$, $d_p = 212 - 250\,\mu m$).

Two subsequent images of the flow, separated by a short time delay, Δt, are divided into small interrogation areas. Cross-correlation analysis is used to determine the displacement of the tracer particles in each interrogation area between the first and second image. The mean tracer velocity in each interrogation area can be then determined since the time delay is known. The

main tasks of image analysis in this case is to discard of bubbles from the subsequent analysis and to enhance the seed particles in the image. Cross-correlation can then be performed by means of commercial softwares or GNU-licensed software (for the present investigation, the MPIV software developed under Matlab by Nobuhito Mori, distributed under GNU - General Public License is adopted).

Fig. 8. Steps of image processing for PIV application to solid particles velocity measurements. From left to right: (a) cropped and ad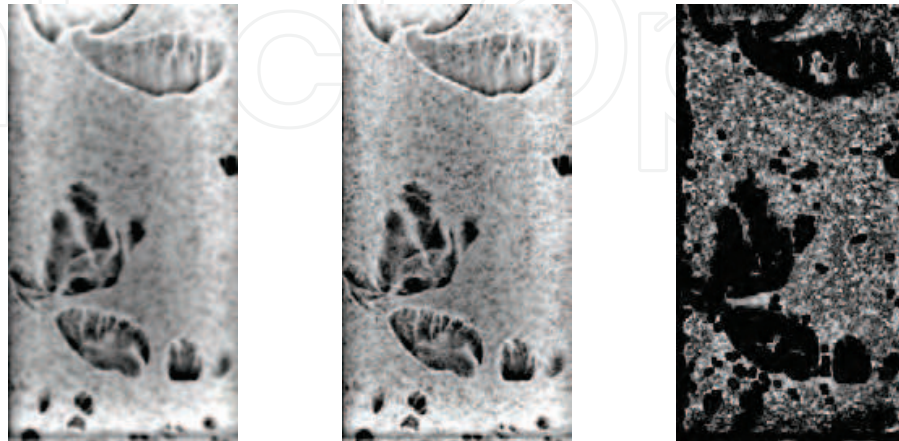justed image; (b) sharpened image; (c) bottom hat transform to minimize illumination non uniformity effects with final bubble elimination.

Bubble identification is needed to neglect particle velocities in highly diluted regions of the bed, *i.e.* inside the gas bubbles. In fact, these regions are characterized by high-particles velocities due to particles spouting from the bubble wake and particle raining from the bubble ceiling. Nevertheless, this velocities belong to few particles with respect to those pertaining to the emulsion phase. On this basis, a reliable measurement of particle velocities have to be restricted to emulsion phase particles. Of course, the seed particle enhancing is needed to make cross-correlation analysis more accurate.

The ideal image for PIV procedure is that in which seed particles give rise to a single illuminated pixel and zero-value pixel otherwise. This is of course a condition very far from the raw images of our system reported in Fig.7. The first step of the image analysis routine consist in the conversion of the acquired image into the relevant greyscale image and relevant exposure adjustment. The result of this operation is reported in Fig.8.a. Notably, bubbles are clearly visible. Then the image is suitably filtered to increase their contrast and increase sharpening, therefore obtaining the image reported in Fig.8.b. Bubbles are then isolated by conversion into a binary images by means of the entropy method (Kapur et al., 1985). At the same time, a bottom-hat morphological transform is applied to the enhanced image, in order to highlight the out-of-background structures. By setting to zero the value of bubble phase-occupied pixels, the final image suitable for PIV procedure is obtained (Fig.8.c). This finally allows the discrimination of bubble phase from the dense phase of the bed and the discrimination of tracer particles.

Then, the images are post processed with the help of the MPIV software under Matlab 7.3 environment. In particular the imaged, is subdivided into a macro areas of $16x16$ pixels,

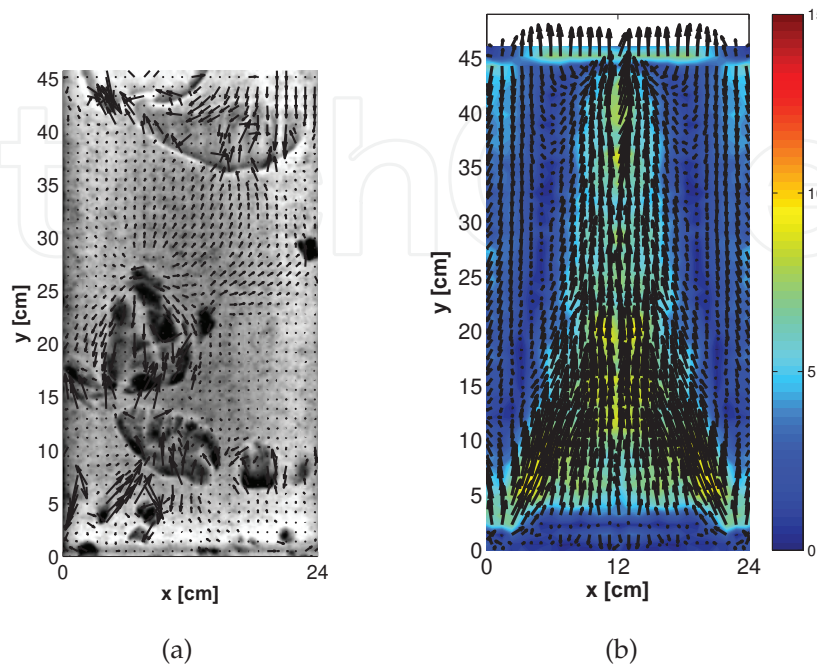and in each area the mean displacement vector of tracer particles along x and y directions is measured.

(a)   (b)

Fig. 9. Typical results of PIV processing (glass particles with corundum tracers, $U = 0.27\,m/s, d_p = 212 - 250\,\mu m$).

In Fig.9.(a), a typical instantaneous velocity field so far obtained is reported, superimposed to the raw image of the system, where it is possible to observe the particle velocity field around each bubble. In Fig.9.(b), the relevant time-averaged velocity plot is reported, highlighting the high-upward mean velocity zone near the center of the bed together with the low-downward mean velocity regions located at the lateral walls.

5. Mixing and segregation dynamics analysis

The fluidization behavior of mixed powder with different diameter or density strongly depends on the nature and composition of the mixture. One of the main characteristics of fluidized mixed powders is the possible onset of segregation or mixing dynamics, depending on inlet gas velocity and particle characteristics. In particular, the heavier (or larger) particles, hereafter referred as jetsam component, show the tendency to segregate toward the bottom of the bed, while the lighter (or smaller), hereafter referred as flotsam component, float above of the segregated particles (Rowe & Yacono, 1975).

The particle mixing characteristics of gas fluidized bed of binary system (i.e. composed of particles with different sizes and/or densities) is of great importance because it is an important factor for the prediction of the bed performance which relates with fluidization quality (Formisani et al., 2008b). Researchers have extensively investigated how dissimilar fluidized particles mix and segregate, aiming at predicting the behavior and understanding the underlying mechanisms of mixing and segregation (Clarke et al., 2007; Formisani et al., 2008a;b). Most of the experimental studies that appear in the literature on polydispersed

fluidized mixtures tried to characterize these systems determining the minimum fluid velocity necessary to fully fluidized them, (Formisani, 1991; Formisani et al., 2001; Noda et al., 1986; Rowe & Yacono, 1976), or studying their dynamics by means of pressure probes (Marzocchella et al., 2000; Olivieri et al., 2004; 2006).

Mostoufi & Chaouki (2000) studied solids behavior by processing the obtained data by a Radioactive Particle Tracking (RPT) technique. In a different paper, the same authors (Mostoufi & Chaouki, 2001) studied the effective diffusivity of solid particles in both bubbling and turbulent regimes. Fennel et al. (2005) used Magnetic Resonance Imaging to studying the rate of axial mixing in a vertical direction of a small plug of solids throughout a fluidized bed of different solids. Humekawa et al. (2005) used X-ray and neutron radiography to studying segregation phenomena. Huang et al. (2008) determined the axial and radial solids dispersion coefficients by a two-dimensional unsteady state dispersion model.

Very few works actually deals with the measurements of segregation or mixing dynamics in bi-dispersed fluidized beds. Leaper et al. (2004) and Bosma & Hoffmann (2003) investigated the dynamics of formation of de-fluidized jetsam layers in fluidized beds, Prasad Babu & Krishnaiah (2005) studied the dynamics of defluidized jetsam layer during segregation of binary heterogeneous mixtures in small continuous-fed reactor. Goldschmidt et al. (2003) developed an experimental technique based on digital image analysis to measure bed expansion and segregation dynamics in dense gas-fluidized beds, in order to validate CFD simulation of mono-disperse and binary mixtures fluid beds. This technique allowed the authors to measure, through the use of differently colored particles and RGB images decomposition, the extent of mixing and segregation. Jang et al. (2010) reported a study on mixing-segregation phenomena in a gas fluidized bed of binary density system performed by analysis of the residence time distribution and mixing degree. The authors also considered axial concentration distribution of jetsam particle and residence time distributions of solids, finally assessing mixing characteristics from the relationship between the residence time and the mixing degree analyzed by sieve test.

In this section we report a new experimental technique, hereafter referred as Mixing and Segregation Dynamics Analysis (Mi.Se.D.A.), based on Digital Image Analysis for the measurement of the mixing behavior in a bi-dispersed 2D fluidized bed.

Corundum particles of different size and colors were used for the present investigation (black corundum particles having $d_p = 212 - 250 \, \mu m$, referred to as flotsam component and white corundum particles having $d_p = 500 - 600 \, \mu m$, referred to as jetsam component). Mixing patterns of the powders were visualized with the aid of a purposely arranged front-lighting device and recorded by a digital camcorder (MVBlueFox). For a better recognition of bubbles, a flat yellow panel was placed in contact with the rear wall of the bed.

Two types of experiments were performed:

• Transient mixing dynamics of segregated powder (jetsam placed at the bottom, flotsam placed at the top of the settled bed).

• Transient segregation dynamics of completely mixed powders.

The technique is based on advanced color images analysis of a bi-dispersed system with powders of different colors. In Fig.10, a typical sequence of snapshots of the bed during mixing experiment is shown. The use of different colored powders allows a clear qualitative recognition of the initial mixed condition and its evolution with time, i.e. the decrease with

time of the settled jetsam layer at the bottom of the bed and the trails of white particles carried by bubbles, especially in the first snapshots. The Image Analysis Technique here proposed is aimed at obtaining quantitative information on the mixing/segregation dynamics. The first problem to tackle is that of recognizing bubbles in the bed, that are clearly detectable by means of visual observation.
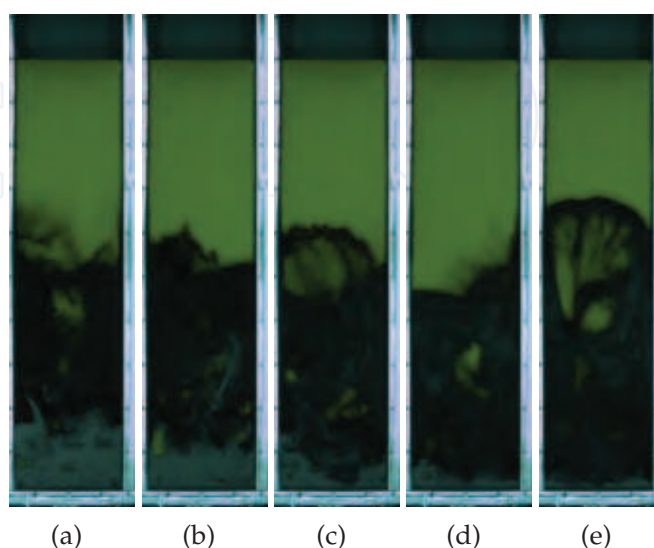

(a)   (b)   (c)   (d)   (e)

Fig. 10. Snapshots of a mixing system taken at $\Delta t = 5\,s$.

The technique is based on a suitable color decomposition of raw images acquired with the above discussed experimental set-up and on subsequent analysis of flotsam concentration dispersion and segregation in a fluidized bed. Two main problems has to be tackled in order to obtain reliable information on mixing or segregation dynamics of powders by means of image analysis:

1. Identification of the solid phase in which composition-related measure must be taken: the images are taken during the vigorous bubbling of the bed, and each color measurement must be limited to pixel belonging to solid phase only;

2. Identification sufficiently reliable relation between image characteristics and bed composition in order to obtain data on the dynamics of bed homogenization or segregation.

It is worth noting that a calibration procedure is not strictly needed when analyzing mixing dynamics, once previously discussed problems are solved. As a matter of fact, it is sufficient to measure a generic quantity monotonically dependent on bed composition to obtain sufficient information on the transitory dynamics from initial to final state of bed homogenization, regardless of the link between actual composition (expressed for example in flotsam weight percentage) and the relevant measure adopted.

Each image is taken and saved by the camera in RGB color space (Red Green Blue), that can be suitably decomposed, as reported in Fig.11(a).

As it can be clearly seen, given the original colors of the adopted powders (near to black and white), each color channel contains similar information. Qualitative analysis of mixing or segregation can be still performed, but such a color decomposition after some trials was found
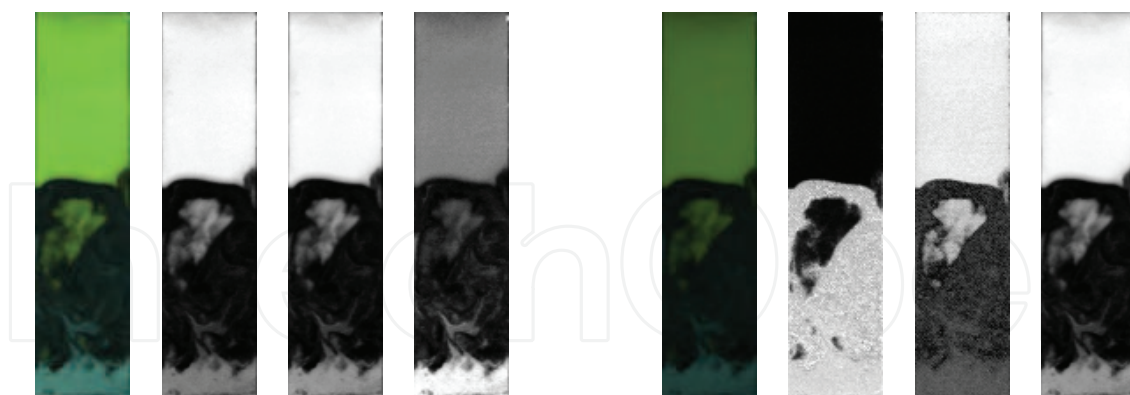
(a) RGB (red, green, blue) decomposition   (b) HSV (hue, saturation, value) decomposition

Fig. 11. Typical original image and intensity plot of relevant decomposed channels in RGB and HSV space, corundum particles in mixing mode, $X = 0.5w/w$ in flotsam component, $U = 0.503\,m/s$.

unsuitable for automatic robust image analysis, even if an example of RGB based process was previously developed (Goldschmidt et al., 2003). It was therefore chosen to adopt a different color space for image analysis, *i.e.* the HSV (Hue, Saturation, Value) color space. Notably HSV is one of the most common cylindrical-coordinate representations of points in an RGB color model, which rearrange the geometry of RGB in an attempt to be more perceptually relevant than the RGB representation itself. The composite image after transformation is of course equal to that previously presented in RGB color space, but its decomposition in single components shows quite different characteristics, as can be observed in Fig.11(b).

As a matter of fact, the hue channel appears to be suitable for the identification of freeboard and bubbles, *i.e.* all bubbles that create a nearly free-of-solid region in the bed that makes yellow panel visible through the bed. A simple threshold value can be chosen by means of entropy method (Kapur et al., 1985) to suitably identify such bubbles. It is therefore possible to generate a logical mask of gas-phase occupied pixels, to be neglected in subsequent analysis of solid phase mixing behavior, as can be seen in Fig.12.

In Fig.12 the relevant distributions of Value in solid phase occupied pixels for a typical experimental case is also reported at two different stages of mixing process. The Value channel was chosen to analyze composition dynamics within the bed, being able to maximize the difference between flotsam and jetsam particles, as already seen in Fig.11(b). This kind of image is somehow proportional to relevant composition map, but, as already discussed, this should not affect mixing or segregation dynamics assessment.

Once the instantaneous Value maps are obtained, the relevant Value distribution can be computed. For the investigated systems, two Value distributions are reported in Fig.12 at two different times. As it is possible to observe for example in Fig.12.(a), in the initial distribution a single peak is observed, because solids are almost uniformly mixed in the early stages of segregation process. Increasing observation time, a strong bimodality clearly occurs in the distribution, because of segregation. Notably, in a fluidized system under mixing conditions,

(a) $t = 0\,s$ (b) $t = 50\,s$
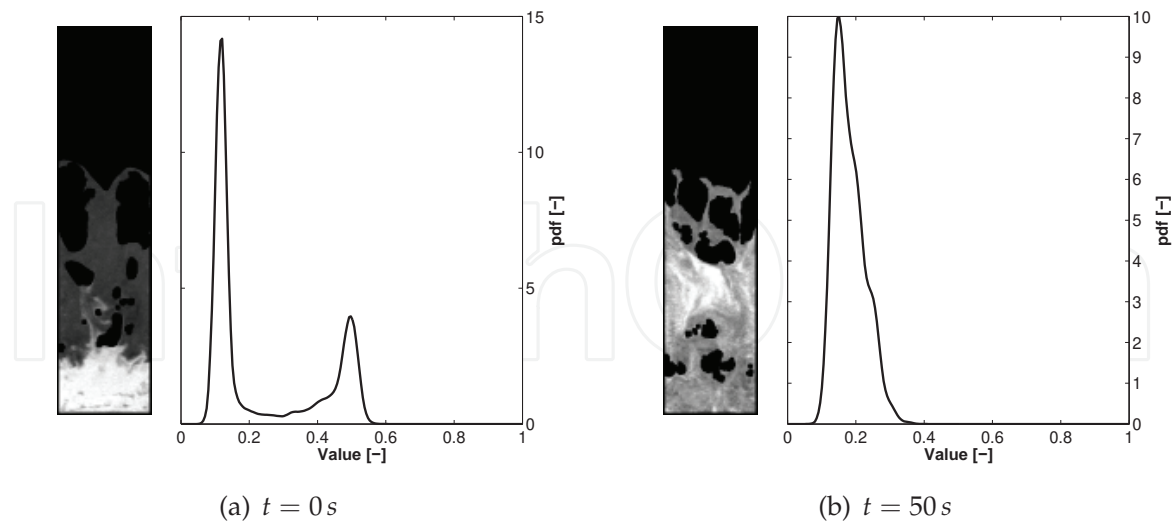
Fig. 12. Value channel with superimposed mask of non-solid phase occupied pixels and relevant distributions of hue values at two different times, corundum particles in mixing mode, $X = 0.5\,w/w$ in flotsam component, $U = 0.503\,m/s$.

the opposite phenomena occurs, *i.e.* a bimodal distribution is found in early stages while a single peak is measured at the end of segregation.

In Fig.13.(a) it is possible to observe the gradual change from a single peaked to a bimodal distribution with time in a segregation experiment. Notably, the steady state reported in Fig.13.(b) highlights that experimental distribution is well fitted with weighted sums of Gaussian distribution.

Notably, the steady state distribution reported shows that a degree of inhomogeneity still exists for both segregated phases. This is likely to be due to both experimental noise and not perfect segregation, but this is not of crucial importance in dynamics measurements.

Conversely, in Fig.14.(a) it is possible to observe the gradual change from a bimodal to a single peaked distribution with time in a mixing experiment. In this case, the steady state distribution reported in Fig.14.(b) has been fitted with a single Gaussian curve that accounts with sufficient accuracy the main characteristics of the experimental distribution. The difference between model and experimental curve is likely to be due to local inhomogeneities still present in the mixed system.

On this basis, a composition chart could be obtained by comparing the parameters of fitted curves (*i.e.* mean value and relevant standard deviation of each peak analyzed) with the known composition of segregated regions and perfectly mixed regions, as shown in Fig.15(a), even if not strictly needed.

As it can be seen, a clear relation can be observed between mean value of mixed powders and composition, that should allow the reconstruction of composition maps from value maps. Nevertheless, the analysis of standard deviations reported in Fig.15(b) shows that the relatively high values of standard deviations (especially for mixed systems, as already discussed), coupled with some low value differences (especially at higher compositions) between segregated flotsam average value and relevant mixed average value does not encourage the translation of Value maps into composition maps, since uncertainties in such
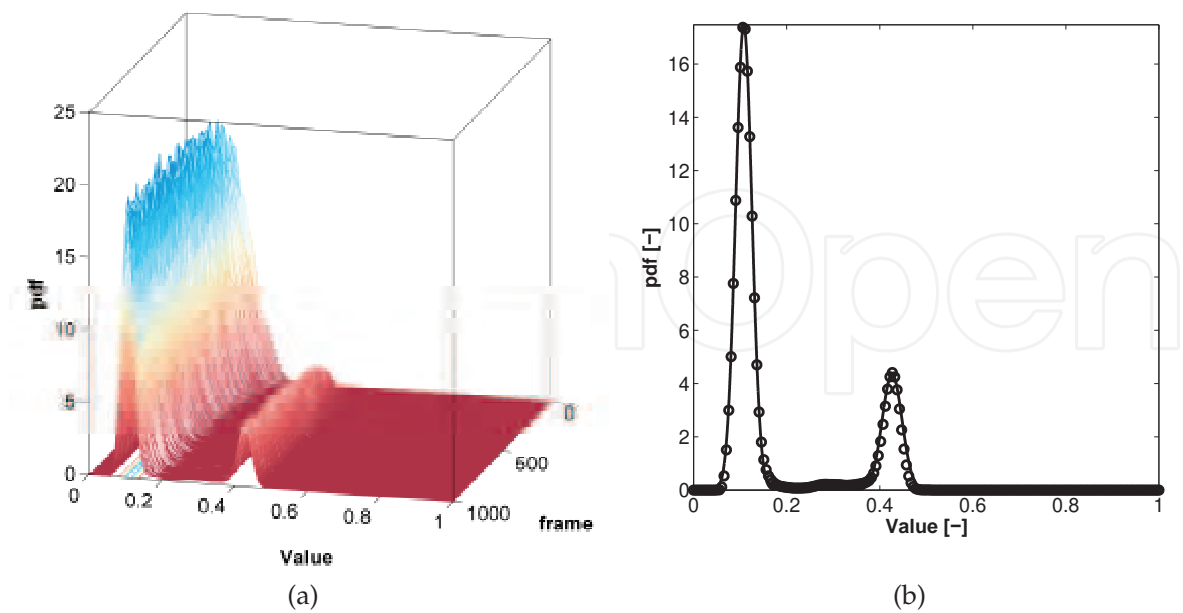
Fig. 13. Value Distribution evolution with time for a segregation experiment ($X = 0.5\,w/w$ in flotsam component, $U = 0.38\,m/s$) and relevant steady state distribution.
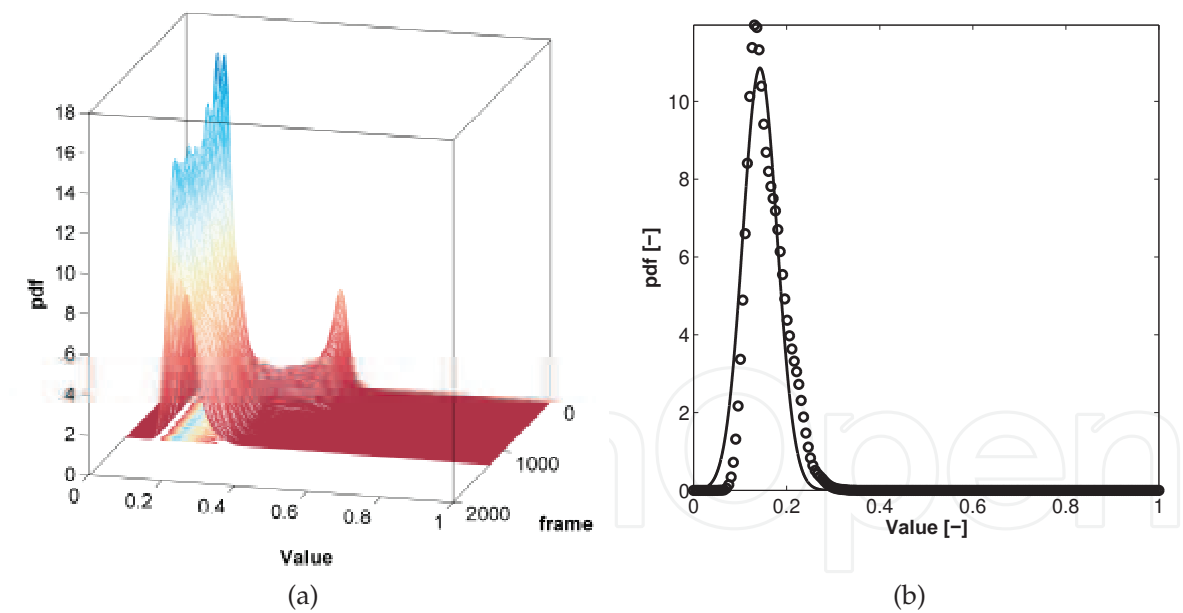
Fig. 14. Value Distribution evolution with time for a mixing experiment ($X = 0.5\,w/w$ in flotsam component, $U = 0.503\,m/s$) and relevant steady state distribution.

a calibration would probably introduce unnecessary errors in the measurements of mixing dynamics.

On this basis, the mixing extent was chosen to be solely measured by means of Value distribution analysis. In particular, the polydispersity index was found to be the best suited to

(a) Mean values

(b) STD values
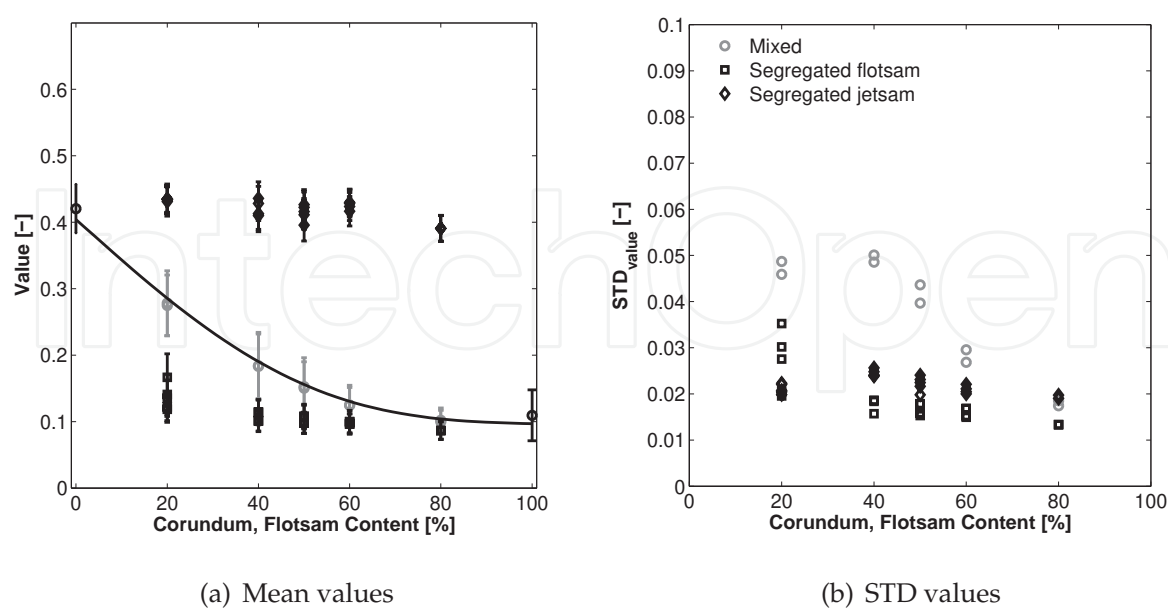
Fig. 15. Value and standard composition chart for all cases.

follow the mixing extent over time. The instantaneous polydispersity index $PI(t)$ of the Value distribution can be readily expressed as the ratio:

$$PI(t) = \frac{\overline{V(t)}_{21}}{\overline{V(t)}_{10}} \tag{8}$$

where the generic average value $\overline{V(t)}_{i,j}$ is simply obtained from the measured Value distribution (pdf) as:

$$\overline{V(t)}_{i,j} = \frac{\int_0^\infty V^i \cdot pdf\,(V)\,\mathrm{d}V}{\int_0^\infty V^j \cdot pdf\,(V)\,\mathrm{d}V} \tag{9}$$

In Fig.16, the typical evolution of polydispersity index as a function of time is shown for the cases of mixing (Fig.16(a)) and segregating (Fig.16(b)) system. Notably, the experimental data show a steep decrease (increase) of PI in the first stages of mixing (segregation), that finally tend to a constant value. It is worth noting the large difference in time scale between mixing end segregation dynamics, the former being in the order of tenth of seconds, the latter in the order of hundreds of seconds. Notably, the deviation from final steady state value can be used to define the mixing time as the time required to cover a variation from initial value of the polydispersity index equal to a known percentage of the whole range. In particular the θ_{95} and θ_{99} times are computed and reported in Fig.16, the former indicating that 95% of the evolution of polydispersity index from initial to final state has been run, the latter indicating a 99% evolution.

The strong difference in mixing and segregation time-scale is substantially a new result, that can be accurately addressed in the future. It is likely to be due to the different mechanism of the phenomena involved, being mixing dynamics mainly bubble-driven and

(a) Mixing, $U = 0.503\,m/s$ (b) Segregation, $U = 0.38\,m/s$
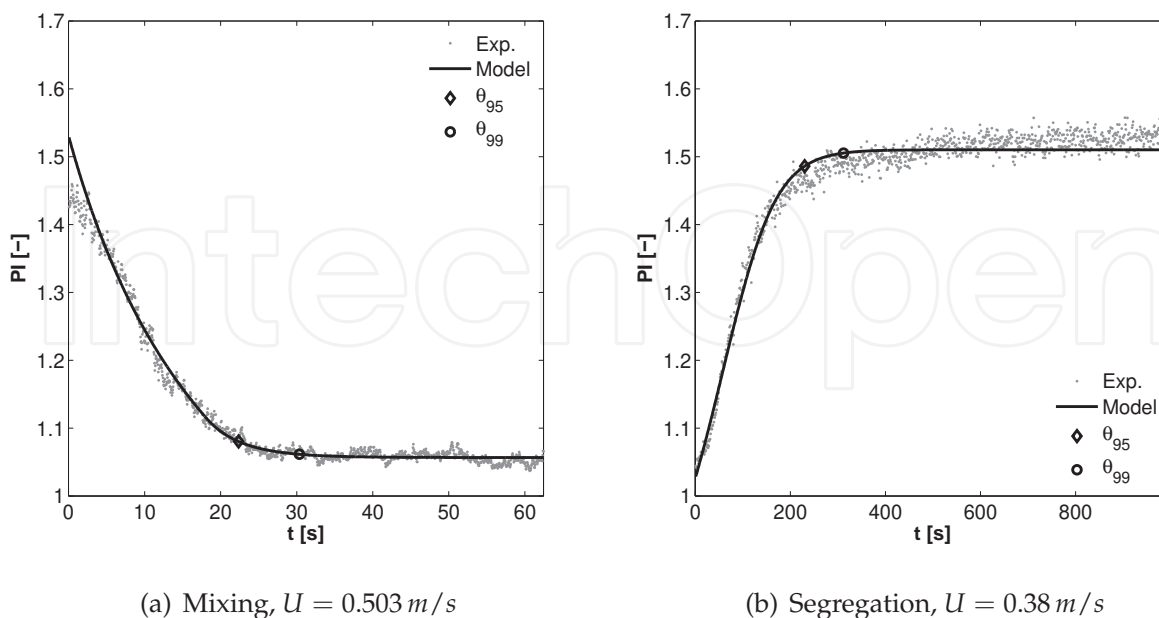
Fig. 16. Examples of polydispersity index evolution with time, $X = 0.5w/w$ in flotsam component.

segregation dynamics linked to slow percolation of jetsam particles through the emulsion phase toward the distributor. Of course, several other experiments have to be performed, and the phenomenon quantified. Notably, these first results were achieved thanks to the Mi.Se.D.A. technique, since the previously adopted techniques for measuring the mixing extent (mainly based on the frozen bed technique, that need the fluid inlet to be stopped and the powder composition analyzed layer by layer) make transient measurements impossible. Conversely, the adoption of image-analysis based techniques allows for the set-up of even large experimental campaigns relatively easy.

6. Conclusions

In this chapter, three different ways of using digital image analysis for fluid dynamic measurements were proposed. All techniques here reported were adopted to study different characteristics of a 2D gas-solid fluidized bed.

Notably, very different quantities can be accurately measured by simply changing illumination set-up and camera settings, ranging from bubble dynamics to solid-phase dynamics.

Image analysis techniques are able to combine ease of measurement, accuracy, non-intrusivity and cost saving.

7. References

Agarwal, G., Lattimer, B., Ekkad, S. & Vandsburger, U. (2011). Influence of multiple gas inlet jets on fluidized bed hydrodynamics using particle image velocimetry and digital image analysis, *Powder Technol.* 214: 122–134.

Agarwal, P., Hull, A. & Lim, K. (1997). *Digital image analysis techniques for the study of bubbling fluidized*, Elsevier, Amsterdam.

Argyriou, D., List, H. & Shinnar, R. (1971). Bubble growth by coalescence in gas fluidized beds, *AIChE J.* 17: 122–130.

Asegehegn, T., Schreiber, M. & Krautz, H. (2011a). Investigation of bubble behavior in fluidized beds with and without immersed horizontal tubes using a digital image analysis technique, *Powder Technol.* 210: 248–260.

Asegehegn, T., Schreiber, M. & Krautz, H. (2011b). Numerical simulation and experimental validation of bubble behavior in 2d gas-solid fluidized beds with immersed horizontal tubes, *Chem. Eng. Sci.* 66: 5410–5427.

Boemer, A., Qi, H. & Renz, U. (1998). Verification of eulerian simulation of spontaneous bubble formation in a fluidized bed, *Chem. Eng. Sci.* pp. 1835–1846.

Bokkers, G., van Sint Annaland, M. & Kuipers, J. (2004). Mixing and segregation in a bidisperse gas-solid fluidized bed: a numerical and experimental study, *Powder Technol.* 140: 176–186.

Bosma, J. & Hoffmann, A. (2003). On the capacity of continuous powder classification in a gas-fluidized bed with horizontal sieve-like baffles, *Powder Technol.* 134: 1–15.

Brucato, A. & Rizzuti, L. (1997a). Simplified modelling of radiant fields in heterogeneous photoreactors. 1. case of zero reflectance, *Ind. Eng. Chem. Res.* 36: 4740–4747.

Brucato, A. & Rizzuti, L. (1997b). Simplified modelling of radiant fields in heterogeneous photoreactors. 2. Limiting two-flux model for the case of reflectance greater than zero, *Ind. Eng. Chem. Res.* 36: 4748–4755.

Busciglio, A., Vella, G., Micale, G. & Rizzuti, L. (2008). Analysis of the bubbling behaviour of 2d gas solid fluidized beds. Part I. Digital Image Analysis Technique, *Chem. Eng. J.* 140: 398–413.

Busciglio, A., Vella, G., Micale, G. & Rizzuti, L. (2009). Analysis of the bubbling behaviour of 2d gas solid fluidized beds. part II. Comparison between experiments and numerical simulations via digital image analysis technique, *Chem. Eng. J.* 148: 145–163.

Busciglio, A., Vella, G., Micale, G. & Rizzuti, L. (2010). Experimental analysis of bubble size distributions in 2D gas fluidized beds, *Chem. Eng. Sci.* 65(16): 4782–4791.

Caicedo, G., Marquéz, J., Ruíz, M. & Soler, J. (2003). A study on the behaviour of a 2D gas-solid fluidized bed using digital image analysis, *Chem. Eng. Process.* 42: 9–14.

Cheremisinoff, N. P. (1986). Review of experimental methods for studying the hydrodynamics of gas-solid fluidized beds, *Ind. Eng. Chem. Process Des. Dev.* 25: 329–351.

Clarke, K., Pugsley, T. & Hill, G. (2007). Fluidization of moist sawdust in binary particle systems in a gasï£¡solid fluidized bed, *Chem. Eng. Sci.* 60: 6909–6918.

Darton, R., LaNauze, R., Davidson, J. & Harrison, D. (1977). Bubble growth due to coalescence in fluidized beds, *Trans. Instn. Chem. Engrs.* 55: 274–280.

Davidson, J., Clift, R. & Harrison, D. (eds) (1985). *Fluidization (2nd Edn.)*, Academic Press, New York USA.

Fennel, P., Davidson, J., Dennis, J., Gladden, L., Hayhurst, A., Mantle, M., Muller, C., Rees, A., Scott, S. & Sederman, A. (2005). A study of the mixing of solids in gas-fluidized beds, using ultra-fast MRI, *Chem. Eng. Sci.* 60: 2085–2088.

Formisani, B. (1991). Packing and fluidisation properties of binary mixtures of spherical particles, *Powder Technol.* 66: 259–264.

Formisani, B., De Cristoforo, G. & Girimonte, R. (2001). A fundamental approach to the phenomenology of fluidization of size segregating binary mixtures of solids, *Chem. Eng. Sci.* 56: 109–119.

Formisani, B., Girimonte, R. & Longo, T. (2008a). The fluidization process of binary mixtures of solids: Development of the approach based on the fluidization velocity interval, *Powder Technol.* 185: 97–108.

Formisani, B., Girimonte, R. & Longo, T. (2008b). The fluidization pattern of density segregating binary mixtures, *Chem. Eng. Res. Des.* 86: 344–348.

Gera, D. & Gautam, M. (1995). Bubble rise velocity in two-dimensional fluidized beds, *Powder Technol.* 84: 283–285.

Goldschmidt, M., Link, J., Mellema, S. & Kuipers, J. (2003). Digital image analysis measurements of bed expansion and segregation dynamics in dense gas-fluidized beds, *Powder Technol.* 138: 135–159.

Hernàndez-Jimènez, F., Sànchez-Delgado, S., Gòmez-Garcìa, A. & Acosta-Iborra, A. (2011). Comparison between two-fluid model simulations and particle image analysis and velocimetry (PIV) results for a two-dimensional gas-solid fluidized bed, *Chem. Eng. Sci.* 66: 3753–3772.

Huang, C., Wang, Y. & Wei, F. (2008). Solid mixing behavior in a nano-agglomerate fluidized bed, *Powder Technol.* 182: 334–341.

Hull, A., Chen, Z., Fritz, J. & Agarwal, P. (1999). Influence of horizontal tube tanks on the behaviour of bubbling fluidized beds. 1. Bubble hydrodynamics, *Powder Technol.* 103: 230–242.

Hulme, I. & Kantzas, A. (2004). Determination of bubble diameter and axial velocity for a polyethylene fluidized bed using X-ray fluoroscopy, *Powder Technol.* 147: 20–33.

Humekawa, H., Furui, S., Oshima, Y., Okura, M., Ozawa, M. & Takenaka, N. (2005). Quantitative measurement of segregation phenomena in a binary-mixture fluidized bed by neutron radiography, *Nuclear Instruments and Methods in Physics research A* 542: 219–225.

Jang, H., Park, T. & Cha, W. (2010). Mixing-segregation phenomena of binary system in a fluidized bed, *Journal of Industrial and Engineering Chemistry* 16: 390–394.

Kapur, J., Sahoo, P. & Wong, A. (1985). A new method for gray-level picture thresholding using the entropy of the histogram, *Comput. Graphics Image Process.* 29: 273–285.

Laverman, J., Roghair, I. & Van Sint Annaland, M. (2008). Investigation into the hydrodynamics of gas-solid fluidized beds using particle image velocimetry coupled with digital image analysis, *Can. J. Chem. Eng.* 86(3): 523–535.

Leaper, M., Seville, J., Hilal, N., Kingman, S. & Burbidge, A. (2004). Investigating the dynamics of segregation of high jetsam binary batch fluidized bed systems, *Chemical Engineering and Processing* 43: 187–192.

Lim, C., Gilbertson, M. & Harrison, A. (2006). Measurement and simulation of bubbling fluidized beds, *Powder Technol.* 170: 167-177.

Lim, C., Gilbertson, M. & Harrison, A. (2007). Bubble distribution and behaviour in bubbling fluidized beds, *Chem. Eng. Sci.* 62: 56–69.

Lim, K. & Agarwal, P. (1990). Conversion of pierced lengths measured at a probe to bubble size measures: an assessment of the geometrical probability approach and bubble shape models, *Powder Technol.* 63: 205–219.

Lim, K. & Agarwal, P. (eds) (1992). *Bubble velocity in fluidized beds: the effect of non-vertical bubble rise on its measurements using submersible probes and its relationship with bubble size*, Vol. 69.

Lim, K., Agarwal, P. & O Neill, B. (1990). Measurement and modelling of bubble parameters in a two-dimensional gas-fluidized bed using image analysis, *Powder Technol.* 60: 159–171.

Lim, K., Agarwal, P. & O'Neill, B. (1993). Mixing of homogeneous solids in bubbling fluidized beds: Theoretical modelling and experimental investigation using digital image analysis, *Chem. Eng. Sci.* 48(12): 2251–2265.

Liu, W. & Clark, N. (1995). Relationship between distributions of chord lengths and distribution of bubble sizes including their statistical parameters, *Int. J. Multiphase flow* 21(6): 1073–1089.

Marzocchella, A., Salatino, P., Di Pastena, V. & Lirer, L. (2000). Transient fluidization and segregation of binary mixtures of particles, *AIChE J.* 46: 2175–2182.

Morooka, S., Tajima, K. & Miyauchi, T. (1972). Behavior of gas bubble in fluid beds, *Int. Chem. Eng.* 12: 168–174.

Mostoufi, N. & Chaouki, J. (2000). On the axial movement of solids in gas-solids fluidized beds, *Trans. IChemE* 78(A): 912–921.

Mostoufi, N. & Chaouki, J. (2001). Local solid mixing in gas solid fluidized beds, *Powder Technol.* 114: 23–31.

Mudde, R., Schulte, H. & van der Akker, H. (1994). Analysis of a bubbling 2-D gas-fluidized bed using image processing, *Powder Technol.* 81: 149–159.

Noda, K., Uchida, S., Makinno, T. & Kamo, K. (1986). Minimum fluidization velocity of binary mixture of particles with large size ratio, *Powder Technol.* 46: 149–154.

Olivieri, G., Marzocchella, A. & Salatino, P. (2004). Segregation of fluidized binary mixtures of granular solids, *AIChE J.* 50: 3095–3106.

Olivieri, G., Marzocchella, A. & Salatino, P. (2006). A fluid-bed continuous classifier of polydisperse granular solids, *Proc. of the 2006 AIChE Spring National Meeting,Orlando, USA*.

Prasad Babu, M. & Krishnaiah, K. (2005). Dynamics of jetsam layer in continuous segregation of binary heterogeneous particles in gas-solid fluidized bed, *Powder Technol.* 160: 114–120.

Rizzuti, L. & Yue, P. (1983). The measurement of light transmission through an irradiated fluidised bed, *Chem. Eng. Sci.* 38(8): 1241–1249.

Rowe, P. & Yacono, C. (1975). The distribution of bubble size in gas fluidized beds, *Trans. Instn. Chem. Engrs.* 53: 59–60.

Rowe, P. & Yacono, C. (1976). The bubbling behaviour of fine powders when fluidised, *Chem. Eng. Sci.* 31: 1179–1192.

Shen, L., Johnsson, F. & Leckner, B. (2004). Digital image analysis of hydrodynamics two-dimensional bubbling fluidized beds, *Chem. Eng. Sci.* 52: 2607–2617.

Sánchez-Delgado, S., Almendros-Ibáñez, J., Soria-Verdugo, A., Santana, D. & Ruiz-Rivas, U. (2008). Coherent structure and bubble-particle velocity in 2-D fluidized beds, *Proceeding of the 9th International Conference on Circulating Fluidized Beds.*, pp. 1007–1012.

Sánchez-Delgado, S., Marugán-Cruz, C., Acosta-Iborra, A. & Santana, D. (2010). Dense-phase velocity fluctuation in a 2-D fluidized bed, *Powder Tech.* 200: 37–45.

van Lare, C., Piepers, H., Schoonderbeek, J. & Thoenes, D. (1997). Investigation on bubble characteristics in a gas fluidized bed, *Chem. Eng. Sci.* 52: 829–841.

Werther, J. (1974a). Bubbles in gas fluidized beds - part I, *Trans. Instn. Chem. Engrs.* 52: 149–159.

Werther, J. (1974b). Bubbles in gas fluidized beds - part II, *Trans. Instn. Chem. Engrs.* 52: 160-169.

Yates, J., Cheesman, d. & Sergeev, Y. (1994). Experimental observations of voidage distribution around bubbles in a fluidized bed, *Chem. Eng Sci.* 49: 1885–1895.

Yue, P., Rizzuti, L. & Augugliaro, V. (1986). Bubble phase voidage and dense phase voidage in thin two dimensional fluidized bed, *Chem. Eng Sci.* 41(1): 171–177.
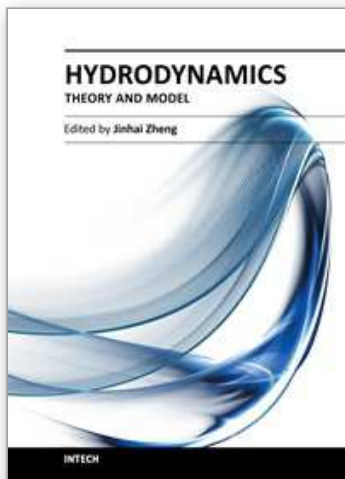
Hydrodynamics - Theory and Model

Edited by Dr. Jin - Hai Zheng

With the amazing advances of scientific research, Hydrodynamics - Theory and Application presents the engineering applications of hydrodynamics from many countries around the world. A wide range of topics are covered in this book, including the theoretical, experimental, and numerical investigations on various subjects related to hydrodynamic problems. The book consists of twelve chapters, each of which is edited separately and deals with a specific topic. The book is intended to be a useful reference to the readers who are working in this field.

How to reference

In order to correctly reference this scholarly work, feel free to copy and paste the following:

Antonio Busciglio, Giuseppa Vella and Giorgio Micale (2012). Measurement of Multiphase Flow Characteristics Via Image Analysis Techniques: The Fluidization Case Study, Hydrodynamics - Theory and Model, Dr. Jin - Hai Zheng (Ed.), ISBN: 978-953-51-0130-7, InTech, Available from:
http://www.intechopen.com/books/hydrodynamics-theory-and-model/measurement-of-multiphase-flow-characteristics-via-image-analysis-techniques-the-fluidization-case-s

INTECH
open science | open minds